



Characteristics of colored dissolved organic matter (CDOM) in the Western Arctic Ocean: relationships with microbial activities

Atsushi Matsuoka, Eva Ortega-Retuerta, Annick Bricaud, Kevin R Arrigo, Marcel Babin

► To cite this version:

Atsushi Matsuoka, Eva Ortega-Retuerta, Annick Bricaud, Kevin R Arrigo, Marcel Babin. Characteristics of colored dissolved organic matter (CDOM) in the Western Arctic Ocean: relationships with microbial activities. Deep Sea Research Part II: Topical Studies in Oceanography, 2015, 118 (Part A), pp.44-52. 10.1016/j.dsr2.2015.02.012 . hal-01120307

HAL Id: hal-01120307

<https://hal.sorbonne-universite.fr/hal-01120307>

Submitted on 25 Feb 2015

HAL is a multi-disciplinary open access archive for the deposit and dissemination of scientific research documents, whether they are published or not. The documents may come from teaching and research institutions in France or abroad, or from public or private research centers.

L'archive ouverte pluridisciplinaire **HAL**, est destinée au dépôt et à la diffusion de documents scientifiques de niveau recherche, publiés ou non, émanant des établissements d'enseignement et de recherche français ou étrangers, des laboratoires publics ou privés.

**Characteristics of colored dissolved organic matter (CDOM) in the Western Arctic
Ocean: relationships with microbial activities**

Atsushi Matsuoka^{1,2,3*}

*Corresponding author

Affiliation 1: *Takuvik* Joint International Laboratory, Département de Biologie, Université Laval,
1045, avenue de la Médecine, Québec, QC, G1V 0A6, Canada
E-mail : Atsushi.Matsuoka@takuvik.ulaval.ca

Phone : +1 (418) 656 2131

Fax : +1 (418) 656 2339

Affiliation 2: *Takuvik* Joint International Laboratory, CNRS, 1045, avenue de la Médecine,
Québec, QC, G1V 0A6, Canada

Affiliation 3: Laboratoire d'Océanographie de Villefranche, Université Pierre et Marie Curie
(Paris 6)/CNRS, B.P. 8, Villefranche-sur-Mer Cedex, 06238, France

Eva Ortega-Retuerta^{1,2,3}

Affiliation 1: Dpt. Biologia Marina i Oceanografia, Institut de Ciències del Mar-CSIC, 08003
Barcelona, Spain

E-mail : ortegaretuerta@icm.csic.es

Phone : +34 93 230 96 06

Fax : +34 93 230 95 55

Affiliation 2: Sorbonne Universités, UPMC Paris 06, UMR 7621, Laboratoire d'Océanographie

27 Microbienne, Observatoire Océanologique, F-66650 Banyuls/mer, France

28

29 Affiliation 3 : CNRS, UMR 7621, Laboratoire d'Océanographie Microbienne, Observatoire

30 Océanologique, F-66650 Banyuls-sur-mer, France

31

32 Annick Bricaud^{1,2}

33 Affiliation 1: Sorbonne Universités, UPMC Paris 06, UMR 7093, LOV, Observatoire

34 Océanographique, F-06230 Villefranche/mer, France

35 E-mail: annick@obs-vlfr.fr

36 Phone : +33 (0)4 93 76 37 13

37 Fax : +33 (0)4 93 76 37 39

38

39 Affiliation 2: CNRS, UMR 7093, LOV, Observatoire Océanographique, F-06230

40 Villefranche/mer, France

41

42 Kevin R. Arrigo

43 Affiliation: Department of Environmental Earth System Science, Stanford University, Stanford,

44 California, 94305, USA

45 E-mail : arrigo@stanford.edu

46 Phone : +1 (650) 723 3599

47 Fax : +1 (650) 498 5099

48

49 Marcel Babin^{1,2,3}

50 Affiliation 1: *Takuvik* Joint International Laboratory, Département de Biologie, Université Laval,

51 1045, avenue de la Médecine, Québec, QC, G1V 0A6, Canada

52 E-mail : Marcel.Babin@takuvik.ulaval.ca

53 Phone : +1 (418) 656 2131

54 Fax : +1 (418) 656 2339

55

56 Affiliation 2: *Takuvik* Joint International Laboratory, CNRS, 1045, avenue de la Médecine,

57 Québec, QC, G1V 0A6, Canada

58

59 Affiliation 3: Laboratoire d'Océanographie de Villefranche, Université Pierre et Marie

60 Curie(Paris 6)/CNRS, B.P. 8, Villefranche-sur-Mer Cedex, 06238, France

61

62 **Abstract**

63 Colored dissolved organic matter (CDOM), a significant fraction of dissolved organic carbon
 64 (DOC), plays various roles in physical and biogeochemical processes in natural waters. In the Arctic
 65 Ocean, CDOM is abundant because of major input by large rivers. To better understand the
 66 processes that drive variations in CDOM, light absorption coefficients of CDOM [$a_{\text{CDOM}}(\lambda)$, m^{-1}]
 67 were extensively documented together with temperature, salinity, chlorophyll *a*, nitrate
 68 concentrations, and bacterial production (BP) and abundance (BA) in the Western Arctic Ocean
 69 (WAO) from early to late summer as part of the MALINA and the ICESCAPE expeditions. The
 70 data set covered contrasting situations, from bloom to post-bloom conditions and from river-
 71 influenced to oceanic water masses. While CDOM photobleaching occurred in the surface layer (<
 72 20 m), we observed significantly lower spectral slopes for CDOM absorption spectra (S_{CDOM}) in
 73 addition to higher $a_{\text{CDOM}}(440)$ in the layer below (intermediate layer: $30.7 < \text{salinity} < 33.9$). In
 74 particular, the low S_{CDOM} values were found in the Chukchi Sea and the western part of the Beaufort
 75 Sea, which coincided with high BP and BA values. Considering the high primary production
 76 observed in these areas during our cruises (Arrigo et al., 2012), we hypothesize that S_{CDOM}
 77 variations reflect the degradation of phytoplankton that is associated with heterotrophic bacterial
 78 activity. In our datasets, a simple regression analysis showed that S_{CDOM} was significantly correlated

with BP and BA. A principal component analysis further supported this conclusion. From our field observations, it was shown that variations in $a_{CDOM}(440)$ and S_{CDOM} result to a large extent from bacterial activity, at least in the WAO.

1. Introduction

Examining the budget of dissolved organic carbon (DOC) in the Arctic Ocean is crucial to improving our understanding of modifications in the carbon cycle resulting from ongoing global warming. While this warming likely induces thawing of permafrost containing a huge amount of DOC, which is subsequently delivered by river discharge into the Arctic Ocean (Peterson et al., 2002; McClelland et al., 2006; Raymond et al., 2007), the long-term trend in the DOC budget of the Pan-Arctic Ocean has yet to be established. In recent studies, Matsuoka et al. (2013, 2014) developed a semi-analytical algorithm to quantitatively estimate DOC concentrations for Arctic coastal waters using satellite remote sensing data, which allows the continuous monitoring of variability in DOC concentrations. In contrast, knowledge about the production and the removal processes gained from field observations using traditional methods is limited temporally and geographically (Bussmann, 1999; Garneau et al., 2008; Kirchman et al., 2009; Ortega-Retuerta et al., 2012). This prevents us from understanding the balance between these processes.

Light absorption by the colored fraction of dissolved organic matter (CDOM) provides useful information about biogeochemical processes (Carder et al., 1989; Nelson et al., 1998; Miller et al., 2002; Nelson et al., 2004, 2007; Matsuoka et al., 2012). While microbial activity is highly variable in natural environments (e.g., Azam et al., 1983), the link between heterotrophic bacterial production and CDOM absorption was reported in the Sargasso Sea (Nelson et al., 1998). More recently, Matsuoka et al. (2012) suggested that lower spectral slopes of CDOM absorption spectra observed in some Arctic Ocean water masses resulted from heterotrophic microbial activity. However, a direct relationship between CDOM and bacteria has not been well documented.

The objective of this study is to examine the relationships between CDOM absorption properties and heterotrophic bacterial production (BP) and abundance (BA) in the Western Arctic Ocean

(WAO) as well as their link with environmental variables (i.e., temperature, salinity, and nitrate and chlorophyll *a* concentrations).

2. Datasets and methods

Data were collected during three cruises in the WAO (Figure 1): the joint France-Canada-USA Arctic campaign, MALINA (30 July to 27 August 2009), and the National Aeronautics and Space Administration (NASA) ICESCAPE cruises in 2010 and 2011 (referred to as ICESCAPE 2010: 15 June to 22 July 2010 and ICESCAPE 2011: 25 June to 29 July 2011, respectively). While waters in the Mackenzie shelf-basin area during the MALINA cruise were oligotrophic and typical of post-bloom conditions (Ortega-Retuerta et al., 2012), waters in the Chukchi-Beaufort Seas during the ICESCAPE cruises were highly productive (Arrigo et al., 2012). To examine the general characteristics in the WAO, these three datasets were combined and used in this study.

Temperature and salinity profiles were obtained using a SBE-911 plus (Seabird) conductivity-temperature-depth (CTD) probe. Chlorophyll *a* (chl *a*) and phaeopigment concentrations (mg m^{-3}) were determined fluorometrically (Holm-Hansen et al., 1965). Nitrate concentrations (NO_3 , $\mu\text{mol kg}^{-1}$) were measured following Grasshoff et al. (1999) for MALINA and Armstrong et al. (1967) for ICESCAPE cruises. Oxygen concentrations (Oxy , $\mu\text{mol kg}^{-1}$) were measured following Carpenter (1965) with modifications by Culberson et al. (1991).

Apparent oxygen utilization (AOU, $\mu\text{mol kg}^{-1}$) was calculated by referring solubility of oxygen for well-mixed winter waters having temperature and salinity of -1.8°C and 31, respectively. These reference data were proven to be valid for western Arctic waters (Matsuoka et al., 2012).

2.1. CDOM absorption

Details of the method used for measurement of CDOM absorption are documented in Matsuoka et al. (2012). Briefly, water samples were filtered using $0.2\ \mu\text{m}$ pore-size filters immediately after sampling. Absorption coefficients of CDOM ($a_{\text{CDOM}}(\lambda)$, m^{-1}) were determined from 200 to 735 nm

in 1-nm increments using a liquid waveguide system (UltraPath, World Precision Instruments, Inc.). The spectral slope of $a_{\text{CDOM}}(\lambda)$ (S_{CDOM} , nm^{-1}) was calculated by nonlinear regression of the data from 350 to 500 nm (Babin et al., 2003; Matsuoka et al., 2011, 2012).

A previous study (Helms et al., 2008) showed that the spectral slopes ($S_{275-295}$ and $S_{350-400}$, nm^{-1} for both) corresponding to two distinct wavelength ranges (i.e., 275-295 nm and 350-400 nm, respectively) and their ratio (S_R , dimensionless) provide insights into sources (e.g., marine or terrestrial sources; Carder et al., 1989; Nelson et al., 2007) and/or local processes affecting the CDOM distribution (e.g., lateral transport, vertical mixing, photo-bleaching, heterotrophic bacterial alteration; Nelson et al., 1998, 2004; Matsuoka et al., 2012; Yamashita et al., 2013). These slope parameters were calculated for our Arctic datasets by fitting a linear model to CDOM absorption coefficients in the two distinct spectral ranges (Helms et al., 2008).

2.2. Bacterial abundance

Heterotrophic prokaryotes, including bacteria and archaea, are abbreviated throughout the manuscript as “bacteria”. Samples were fixed with glutaraldehyde (0.25% final concentration) and stored at -80°C until processing. During MALINA, bacterial cells (BA) were counted aboard the ship by flow cytometry using a FACS ARIA (Becton, Dickinson and company) equipped with 488 nm and 633 nm lasers and a standard filter setup (Ortega-Retuerta et al., 2012). During ICESCAPE 2010, bacterial cells were counted by flow cytometry at the home laboratory using a BD FACS Calibur Flow Cytometer (Becton, Dickinson and company). During ICESCAPE 2011, bacterial cells were counted aboard the ship using an Accuri C6 (Becton, Dickinson and company) equipped with a 488 nm laser. In all cases, samples were thawed and SYBR Green-I was added at a final dilution of 1:10,000. Samples were incubated in the dark for 15 min before analysis. Bacterial cells were identified on a plot of green fluorescence (515-545 nm) versus right angle light scatter (SSC), using the green fluorescence as a threshold parameter. High nucleic acid (HNA) and low nucleic acid (LNA) bacteria were discriminated according to their green fluorescence and counted

separately (Marie et al., 1997). HNA cells have often been considered as active bacteria (Gasol et al., 1999).

2.3. Bacterial production

Bacterial production (BP) was measured following Ortega-Retuerta et al. (2012). Briefly BP was measured by ^3H -leucine incorporation (Smith and Azam, 1992). Samples (1.5 mL in triplicate plus one killed control) were added to sterile microcentrifuge tubes, containing 20-30 nM [4,5- ^3H]-leucine. This concentration was sufficient to saturate bacterial leucine uptake (data not shown). Incorporation rates were measured after 2-h incubations at *in situ* temperature, and incubations were stopped by the addition of trichloroacetic acid (5% final concentration). Leucine incorporation rates were converted to carbon production using the conversion factor of 1.5 kg C produced per mole of leucine incorporated (Kirchman, 1993), considering no isotope dilution.

2.4. Statistical analyses

2.4.1. Regression analysis

To examine a direct relationship between two variables, several regression analyses were performed. Because the two variables were random (or not controlled), Model II regression was applied in this study (Legendre and Legendre, 1998).

2.4.2. Principal component analysis

For a dataset containing several variables, a multiple regression analysis is not always the best method for examining the relationships among the variables. Principal component analysis (PCA) is preferable because it summarizes, in a few dimensions, most of the variability present in a dispersion matrix of a large number of variables (Legendre and Legendre, 1998), and has been applied to a large number of oceanographic studies (e.g., Legendre and Legendre, 1998; Uitz et al., 2008; Suzuki et al., 2012). We thus applied this method to our datasets.

183

184 2.5. Sea ice concentration

185 Daily sea ice concentrations data acquired by the Defense Meteorological Satellite Program
186 (DMSP) SSM/I passive microwave sensor (25-km spatial resolution) were downloaded from the
187 National Snow and Ice Data Center (NSIDC) at
188 ftp://sidacs.colorado.edu/pub/DATASETS/nsidc0051_gsfc_nasateam_seaice/. Daily images (29 for
189 MALINA, 38 for ICESCAPE2010, and 35 for ICESCAPE2011) were averaged to generate an
190 image of mean sea ice concentrations for each cruise (Figure 2).

191

192 3. Results and discussion

193 3.1. Vertical distribution of CDOM

194 To examine the vertical distribution of CDOM absorption properties in the WAO, $a_{CDOM}(440)$
195 and S_{CDOM} were plotted against depth (Figure 3). At depth < 150 m, $a_{CDOM}(440)$ values were highly
196 variable for early to middle summer (ICESCAPE2010 and 2011 data: blue crosses and red
197 diamonds in Figure 3a and c). Values for late summer (MALINA data: black circles in Figure 3a),
198 however, were less variable and low near the surface (down to 0.0197 m^{-1}), except for river waters
199 that showed significantly higher values (up to 1.08 m^{-1} ; see arrow in Figure 3a). At depth > 150 m,
200 all data tended to decrease with depth, approaching $0.0277 \pm 0.0025 \text{ m}^{-1}$ (dotted rectangle in Figure
201 3c). This type of profile was similar to that reported by Guéguen et al. (2012), who suggested that
202 the maximal values around 150 m are associated with microbial activity (see sections 3.3 and 3.4).
203 While determination of the origin of CDOM (e.g., production by phytoplankton, heterotrophic
204 bacteria, etc) is still challenging using our dataset alone, we acknowledge that phytoplankton
205 especially at the deep chlorophyll maximum is one of the CDOM sources (Matsuoka et al, 2012).

206 Similarly to $a_{CDOM}(440)$, S_{CDOM} values for early-middle summer varied widely at depths < 150
207 m (Figure 3b). In contrast, those values showed less variability in late summer and were highest
208 near the surface (up to 0.022 nm^{-1} ; Figure 3b and d). At depths > 150 m, all S_{CDOM} values

approached $0.0167 \pm 0.0005 \text{ nm}^{-1}$ with increasing depth (dotted rectangle in Figure 3d).

For surface waters, our results thus showed that $a_{\text{CDOM}}(440)$ values decreased in association with increases in S_{CDOM} from early to late summer (for up to 2.5 months). It is well known that as a result of solar irradiation, high-weight molecules are transported into low-weight molecules that absorb light in the shorter spectral wavelengths, a phenomenon called photo-bleaching. The spectral slope therefore increases after the photo-bleaching (Twardowski and Donaghay, 2002). The timescale is likely one to three months (Granskog et al., 2009). Satellite-derived sea ice concentration images further showed that surface waters at most of our sampling stations were ice-free and therefore exposed to solar irradiation (Figure 2). All these results demonstrate photo-bleaching occurred during our observations.

For deep waters, CDOM absorption properties were stable (Figure 3a and b). Because CDOM in these waters is considered to be biologically unavailable or refractory, those absorption values can be considered as an end-member for refractory CDOM. If so, the proportion of CDOM lability could be optically quantified when the other end-member from labile CDOM is obtained. Further work is necessary to examine this issue.

3.2. Relationship between CDOM and hydrography

Because salinity can be a good proxy of Arctic Ocean hydrography (e.g., Carmack et al., 1989; Macdonald et al., 1989; Matsuoka et al., 2012), relationships between CDOM absorption properties (i.e., $a_{\text{CDOM}}(440)$ and S_{CDOM}) and salinity were examined (Figure 4). At salinity < 28 , two types of waters were distinguished: 1) river waters with a strong negative correlation between $a_{\text{CDOM}}(440)$ and salinity and 2) ice-melt waters showing both low $a_{\text{CDOM}}(440)$ and salinity (Figure 4a; see also Matsuoka et al., 2012). These waters were observed in the Mackenzie shelf-basin area in the late summer (black circles: MALINA cruise); river waters samples were collected in the Mackenzie River mouth, while ice melt waters samples were taken near the sea ice, far away from the river mouth ($> 300 \text{ km}$). Data points at salinities < 28 located in the Chukchi-Beaufort Seas in mid-

summer (red diamonds: ICESCAPE 2011 cruise) were not far away from the negative $a_{CDOM}(440)$ versus salinity relationship for MALINA cruise (Figures 4a and b). In this salinity range, S_{CDOM} exhibited low variability (0.0196 ± 0.0011 ; Figure 4b), which is consistent with the value reported by Matsuoka et al. (2012) (0.0192 ± 0.0011).

At salinities > 28 , $a_{CDOM}(440)$ values for the MALINA cruise tended to be lower than those for the ICESCAPE 2010&2011 cruises (early-middle summer) conducted in the Chukchi-Beaufort Seas (Figure 4c). This was especially true in the surface layer (i.e., $28 < \text{salinity} < 30.7$), where the lower $a_{CDOM}(440)$ values for the MALINA cruise corresponded to slightly but significantly higher S_{CDOM} values (0.0189 ± 0.0006) compared to those for the ICESCAPE 2010&2011 cruises (0.0182 ± 0.0004 and 0.0183 ± 0.0012 , respectively) (T-test, $p < 0.0001$; Figure 4c and d), which suggests that photo-bleaching occurred from early-middle to late summer (Nelson et al., 1998; Twardowski and Donaghay, 2002, Matsuoka et al., 2011; see also Figure 3). In other words, CDOM in the Chukchi-Beaufort Seas observed during the early-middle summer cruises might have been relatively *new* because of *in situ* production and/or input from the Bering Sea (Matsuoka et al., 2011; Shen et al., 2012).

The negative relationship between $a_{CDOM}(440)$ and salinity in the Lower Halocline Water (LHW: $33.9 < \text{salinity} < 34.7$) and Atlantic Layer (AL: salinity > 34.7 ; our water samples were always collected at depths shallower than 850 m) was very similar among cruises (Figure 4c). This relationship was likely stable across ice-free seasons and areas of the WAO. So the $a_{CDOM}(440)$ versus salinity relationship could be specific to these waters.

In the intermediate layer between the surface and the LHW+AL layers (i.e., $30.7 < \text{salinity} < 33.9$), $a_{CDOM}(440)$ values for the ICESCAPE 2010&2011 cruise in the Chukchi-Beaufort Seas were significantly higher than those for MALINA in the Mackenzie shelf-basin area (T-test, $p < 0.0001$). Correspondingly, S_{CDOM} values in the intermediate layer were much lower for the ICESCAPE 2010&2011 cruises than for the MALINA cruise (T-test, $p < 0.0001$; Figure 4d). Based on field observations, Nelson et al. (1998) suggested that bacteria produce CDOM when taking up dissolved

organic carbon (DOC), which is also consistent with results from laboratory experiments. Moran et al. (2000), Helms et al. (2008), and Ortega-Retuerta et al. (2009) observed that heterotrophic bacterial activity is associated with a decrease in the spectral slope of CDOM absorption over time. Note, however, that this result is contrary to the one obtained by Nelson et al., 2004. This contrast might originate from differences in substrate of organic matter utilized by bacteria and/or in distinct bacterial assemblages. Considering these findings, we hypothesized that the significantly low S_{CDOM} values observed in this study are associated with heterotrophic microbial activity.

To test this hypothesis, a vertical section of CDOM absorption properties, as well as salinity and phaeopigments in the intermediate layer (i.e., $30.7 < \text{salinity} < 33.9$), along the transect from the Kotzebue Sound (KS) to the Chukchi Hotspot (CH) was further analyzed (Figure 5). The transect covered both river-influenced and biologically productive areas sampled during the ICESCAPE 2010 cruise (see Figure 1 for location). Waters showing high $a_{CDOM(440)}$ and low salinity values were observed in the surface layer of the KS, indicating river-influenced waters (Figure 5a and b). Further offshore, this trend was no longer observed in the surface layer of the CH. Relatively high $a_{CDOM(440)}$ values, corresponding to significantly low S_{CDOM} values, were observed near the bottom of the CH. Interestingly, the low S_{CDOM} values were associated with high concentrations of phaeopigments ($r^2 = 0.70$, $p < 0.0001$; Figure 5c and d); BP measurements are not shown here because of the limited number of data points along this transect. Because phaeopigments reflect degradation products of phytoplankton intermediated by bacteria, this result partly supports our hypothesis that both the high $a_{CDOM(440)}$ and low S_{CDOM} values observed in this study resulted from heterotrophic microbial activity.

3.3. Relationship between the spectral slope of CDOM absorption and bacteria

To examine the direct relationship between the spectral slope of CDOM absorption and bacteria, S_{CDOM} was regressed against BP and BA (Figure 6; chl *a* concentrations, temperature and nitrate concentrations were also regressed against S_{CDOM}). There was a weak but significant negative

correlation between BP and S_{CDOM} (Figure 6a; $r^2 = 0.20$, $p < 0.0001$). The coefficient of determination for this relationship was the second highest following the BP versus chl a relationship ($r^2 = 0.24$, $p < 0.0001$; Table 1). Temperature showed the third highest correlation with slightly lower coefficient of determination ($r^2 = 0.18$, $p < 0.0001$). Significant correlations were not found for BP versus salinity or nitrate concentrations.

S_{CDOM} was negatively correlated with BA (Figure 6b; $r^2 = 0.26$, $p < 0.0001$). The coefficient of determination for this relationship was the highest, followed by BA versus chl a ($r^2 = 0.22$, $p < 0.0001$; Table 1). Similarly to BP, temperature showed the third highest correlation with BA ($r^2 = 0.17$, $p < 0.0001$). No significant correlations were found between BA and either salinity or NO_3 concentration. These results suggest that low S_{CDOM} values were generally associated with high BP and BA in our environments.

A similar regression analysis was performed for the spectral parameters $S_{275-295}$, $S_{350-400}$, and S_R , as done by Helms et al. (2008). Although results using $S_{350-400}$ were similar to those using S_{CDOM} (Table 2), none of them revealed higher correlations with BP and BA than S_{CDOM} ; S_{CDOM} is a better variable to reflect bacterial activity.

3.4. Multiple relationships among variables

To examine relationships among several variables, a PCA analysis was performed. The extracted axes of the PCA (Figure 7) can be interpreted as follows. Principal Component 1 (PC1) made the largest contribution, explaining 30.9 % of total variance. The positive component was strongly related to chl a , $a_{CDOM}(440)$, BA, and BP and had a weak relationship with temperature and salinity. Thus, the positive PC1 was considered to reflect production of organic matter. More interestingly, S_{CDOM} alone showed the opposite trend compared to the above-mentioned variables (i.e., production of organic matter), suggesting that negative PC1 might reflect the decomposition of organic matter.

Principal Component 2 (PC2) explained 21.4 % of total variance. The negative component was strongly related to NO_3 concentration and apparent oxygen utilization (AOU) and was weakly

related to salinity. NO_3 and AOU were tightly correlated, consistent with recent findings by Matsuoka et al. (2012) for these two variables in the salinity range of 30.7-33.9 (or approximately 50-200 m depth; see their Figures 3c and d). Thus, negative PC2 was considered to reflect the aphotic zone. In contrast, the positive PC2 might reflect the euphotic zone, which is further supported by the fact that this component was weak but related to the production of organic matter.

Note that result of salinity in the PCA analysis is not surprising and can be explained as follows. First, salinity exhibited an opposite trend compared to that shown by S_{CDOM} . This general trend is shown in Figure 4. Second, this variable had a negative direction in PC2. This result is consistent with our discussion that negative PC2 represents the aphotic zone, showing higher salinity. Furthermore, Figure 7 provides important information: Because only S_{CDOM} showed opposite direction compared to parameters related to production of organic matter, this variable might be considered to reflect the degradation products of organic matter.

As expected, S_{CDOM} was negatively correlated with BP and BA (Figure 6), which is consistent with the result of simple regression analysis (Figure 6 and Table 1). Similarly, S_{CDOM} was negatively correlated with chl *a* and phaeopigments ($p < 0.0001$ for both). By taking into account the findings in Figures 5-7, our results suggest that variations in S_{CDOM} reflect the degradation of phytoplankton that is associated with heterotrophic bacterial activity.

4. Conclusions

This study demonstrated that variations in the spectral slope of CDOM absorption (S_{CDOM}) are partly explained by bacterial production (BP) and bacterial abundance (BA) variations. A simple regression analysis showed that S_{CDOM} was related to both BA and BP, which was further supported by PCA analysis. Bacterial abundance and production is likely dependent on bioavailability of DOM (e.g., Moran et al., 2000; Helms et al., 2008; Ortega-Retuerta et al., 2009). The spectral slope of CDOM reflects to some extent the level of DOC availability (Moran et al., 2000; Helms et al., 2008; Ortega-Retuerta et al., 2009). Therefore, it is consistent that S_{CDOM} is significantly correlated

with bacterial activity. Further work is necessary to better understand changes in CDOM cycling in the Arctic Ocean.

Acknowledgements

We are grateful to the captain and crews of the Canadian Icebreaker *CCGS Amundsen* and the US icebreaker *USCGC Healy*. CTD deployment and data processing were made by Y. Gratton, L. Prieur, and C. Marec for MALINA and J. Swift and R. S. Pickart for ICESCAPE cruises. Water samples from a small boat were provided by S. B. Hooker. Fluorometric chlorophyll *a* concentrations were measured by S. Bélanger and A. Mignot for MALINA and K. R. Arrigo, M. Mills, G. van Dijken, Z. Brown, M. Palmer, and K. Lowry for ICESCAPE cruises. Nitrate concentrations were provided by J. E. Tremblay, P. Raimbault, N. Garcia, and J. Gagnon for MALINA and S. Becker for ICESCAPE cruises. Technical supports by Q. Allison, S. Tolley, S. Hiller, S. Laney, and S. Roberts are much appreciated. Bacterial abundance and production data during MALINA were kindly provided by D. Marie, F. Joux and W.H. Jeffrey. Comments from two anonymous reviewers greatly improved the manuscript. This study was conducted as part of the MALINA Scientific Program funded by ANR (Agence nationale de la recherche), INSU-CNRS (Institut national des sciences de l'univers – Centre national de la recherche scientifique), CNES (Centre national d'études spatiales) and ESA (European Space Agency). This research was also supported by the Ocean Biology and Biogeochemistry Program and the Cryosphere Science Program of the National Aeronautic and Space Administration (NNX10AF42G to K. Arrigo). We also thank a joint contribution to the research programs of UMI Takuvik, ArcticNet (Network Centres of Excellence of Canada) and the Canada Excellence Research Chair in Remote Sensing of Canada's New Arctic Frontier.

References

Armstrong, F.A. Stearns, J., C. R., and Strickland, J. D. H., 1967, The measurement of upwelling

- 365 and subsequent biological processes by means of the Technicon AutoAnalyzer™ and
- 366 associated equipment. *Deep-Sea Res.* 14(3): 381-389.
- 367 Arrigo, K. R., Perovich, D.K., Pickart, R.S., Brown, Z.W., van Dijken, G.L., Lowry, K.E., Mills,
- 368 M.M., Palmer, M.A., Balch, W.M., Bahr, F., Bates, N.R., Benitez-Nelson, C., Bowler, B.,
- 369 Brownlee, E., Ehn, J.K., Frey, K.E., Garley, R., Laney, S.R., Lubelczyk, L., Mathis, J.,
- 370 Matsuoka, A., Mitchell, B.G., Moore, G.W.K., Ortega-Retuerta, E., Pal, S., Polashenski,
- 371 C.M., Reynolds, R.A., Schieber, B., Sosik, H.M., Stephens, M., and Swift, J.H., 2012,
- 372 Massive Phytoplankton Blooms Under Arctic Sea Ice, *Science*, 10.1126/science.1215065.
- 373 Azam, F., Fenchel, T., Field, J.G., Gray, J.S., Meyer-Rei, L.A., and Thingstad F., 1983, The
- 374 Ecological Role of Water-Column Microbes in the Sea, *Mar. Ecol. Prog. Ser.*, 10, 257-263.
- 375 Babin, M., Stramski, D., Ferrari, G. M., Claustre, H., Bricaud, A., Obolensky, G., and Hoepffner,
- 376 N., 2003, Variations in the light absorption coefficients of phytoplankton, nonalgal particles,
- 377 and dissolved organic matter in coastal waters around Europe, *J. Geophys. Res.*, 108,
- 378 doi:10.1029/2001JC00082.
- 379 Bussmann, I., 1999, Bacterial utilization of humic substances from the Arctic Ocean, *Aquat. Microb.*
- 380 *Ecol.*, 19, 37-45.
- 381 Carmack, E.C., Macdonald, R.W., and Papadakis, J.E., 1989, Water mass structure and boundaries
- 382 in the Mackenzie shelf estuary, *J. Geophys. Res.*, 94, 18043–18055.
- 383 Carder, K.L., Steward, R.G., Harvey, G.R., and Ortner, P.B., 1989, Marine humic and fulvic
- 384 acids: Their effects on remote sensing of ocean chlorophyll, *Limnol. Oceanogr.*, 34, 68–81.
- 385 Carpenter, J.H., 1965, The accuracy of the Winkler method for dissolved oxygen, *Limnol.*
- 386 *Oceanogr.*, 10, 135-140.
- 387 Culberson, C.H., 1991, Dissolved Oxygen, WHP Operations and Methods, Unpublished manuscript,
- 388 15 pp.
- 389 Ducklow, H.W., 1992, Factors regulating bottom-up control of bacterial biomass in open ocean
- 390 plankton communities, *Ergeb. Limnol.*, 37, 207–217.

- 391 Garneau, M.-E., Roy S., Lovejoy, C., Gratton, Y., and Vincent W.F., 2008, Seasonal dynamics of
 392 bacterial biomass and production in a coastal arctic ecosystem: Franklin Bay, western
 393 Canadian Arctic, *J. Geophys. Res.*, 113, C07S91, doi:10.1029/2007JC004281.
- 394 Gasol, J.M., Zweifel, U.L., Peters, F., Fuhrman, J.A., Hagstrom, A., 1999, Significance of size and
 395 nucleic acid content heterogeneity as measured by flow cytometry in natural planktonic
 396 bacteria. *Appl. Environ. Microbiol.* 65, 4475-4483.
- 397 Guéguen, C. McLaughlin, F. A., Carmack, E. C., Itoh, M. Narita, H., and Nishino, S., 2012, The
 398 nature of colored dissolved organic matter in the southern Canada Basin and East Siberian
 399 Sea, *Deep-Sea Res.*, II, 81-84, 102-113.
- 400 Granskog, M., Macdonald, R. W., Kuzyk, Z. Z. A., Senneville, S., Mundy, C.-J., Barber, D., Stern,
 401 G. A., and Saucier, F., 2009, Coastal conduit in southwestern Hudson Bay (Canada) in
 402 summer: Rapid transit of freshwater and significant loss of colored dissolved organic matter,
 403 *J. Geophys. Res.*, 114, C08012, doi:10.1029/2009JC005270.
- 404 Grasshoff, K., Kremling, K. and Ehrhardt, M. (Eds.), 1999, *Methods of seawater analysis*, New
 405 York, Wiley-VCH.
- 406 Helms, J.R., Stubbins, A., Ritchie, J.D., Minor, E.C., Kieber, D. J., and Mopper, K., 2008,
 407 Absorption spectral slopes and slope ratios as indicators of molecular weight, sources, and
 408 photobleaching of chromophoric dissolved organic matter, *Limnol. Oceanogr.*, 53, 955–
 409 969.
- 410 Holm-Hansen, O., Lorenzen, C.J., Holmes, R.W., and Strickland, J.D.H., 1965, Fluorometric
 411 Determination of Chlorophyll, *J. Cons. perm. int. Explor. Mer.*, 30, 3-15.
- 412 Kirchman, D.L., Moran, X.A.G., and Ducklow, H., 2009, Microbial growth in the polar oceans –
 413 role of temperature and potential impact of climate change, *Nature Rev.*, 7, 451-459.
- 414 Kirchman, D.L., 1993, Leucine incorporation as a measure of biomass production by heterotrophic
 415 bacteria, in: PF, K. (Ed.), *Handbook of methods in aquatic microbial ecology*. Lewis
 416 Publishers, Boca Raton, pp. 509-512.

- 417 Legendre, P., and Legendre, L., 1998, Numerical Ecology, New York.
- 418 Marie, D., Partensky, F., Jacquet, S., Vaulot, D., 1997, Enumeration and cell cycle analysis of
- 419 natural populations of marine picoplankton by flow cytometry using the nucleic acid stain
- 420 SYBR Green I. Appl. Environ. Microbiol. 63, 186-193.
- 421 Matsuoka, A., Bricaud, A., Benner, R., Para, J., Sempere, R., Prieur, L., Bélanger, S., and Babin, M.,
- 422 2012, Tracing the transport of colored dissolved organic matter in water masses of the
- 423 Southern Beaufort Sea: relationship with hydrographic characteristics, Biogeosciences, 9,
- 424 doi: 10.5194/bg-9-925-2012.
- 425 Matsuoka, A., Hill, V., Huot, Y., Bricaud, A., and Babin, M., 2011, Seasonal variability in the light
- 426 absorption properties of western Arctic waters: parameterization of the individual
- 427 components of absorption for ocean color applications, J. Geophys. Res., 116,
- 428 doi:10.1029/2009JC005594.
- 429 Matsuoka, A., Hooker, S.B., Bricaud, A., Gentili, B., and Babin, M., 2013, Estimating absorption
- 430 coefficients of colored dissolved organic matter (CDOM) using a semi-analytical algorithm
- 431 for southern Beaufort Sea waters: applications to deriving concentrations of dissolved
- 432 organic carbon from space, Biogeosciences, 10, doi: 10.5194/bg-10-917-2013.
- 433 Matsuoka, A., Babin, M., Doxaran, D., Hooker, S.B., Mitchell, B.G., Bélanger, S., and Bricaud, A.,
- 434 2014, A synthesis of light absorption properties of the Arctic Ocean: application to semi-
- 435 analytical estimates of dissolved organic carbon concentrations from space, Biogeosci., 11,
- 436 3131-3147, doi:10.5194/bg-11-3131-2014.
- 437 Macdonald, R.W., Carmack, E.C., McLaughlin, F.A., Iseki, K., Macdonald, D.M., and O'Brien,
- 438 M.C., 1989, Composition and modification of water masses in the Mackenzie shelf estuary,
- 439 J. Geophys. Res., 94, 18057–18070.
- 440 McClelland, J.W., Déry, S.J., Peterson, B.J., Holmes, R.M., and Wood, E.F., 2006, A pan-arctic
- 441 evaluation of changes in river discharge during the latter half of the 20th century, Geophys.
- 442 Res. Lettr., 33, L06715, doi:10.1029/2006GL025753.

- 443 Moran, M.A., Sheldon, W. M. Jr., and Zepp, R. G., 2000, Carbon loss and optical property changes
 444 during long-term photochemical and biological degradation of estuarine dissolved organic
 445 matter, *Limnol. Oceanogr.*, 45(6), 1254-1264.
- 446 Miller, W.L., Moran, M.A., Sheldon, W.M., Zepp, R.G., and Opsahl, S., 2002, Determination of
 447 apparent quantum yield spectra for the formation of biologically labile photoproducts,
 448 *Limnol. Oceanogr.*, 47, 343–352.
- 449 Nelson, N.B., Siegel, D.A., Michaels, A.F., 1998, Seasonal dynamics of colored dissolved
 450 material in the Sargasso Sea, *Deep Sea Research Part 1*, 45, 931-957.
- 451 Nelson, N. B., Carlson, C. A., and Steinberg, D. K., 2004, Production of chromophoric dissolved
 452 organic matter by Sargasso Sea microbes, *Mar. Chem.*, 89, 273-287.
- 453 Nelson, N.B., Siegel, D.A., Carlson, C.A., Swan, C., Smethie, W.M. Jr., and Khatiwala, S., 2007,
 454 Hydrography of chromophoric dissolved organic matter in the North Atlantic, *Deep Sea*
 455 *Research Part 1*, 54, 710-731.
- 456 Ortega-Retuerta, E., Jeffrey, W.H., Babin, M., Bélanger, S., Benner, R., Marie, D., Matsuoka, A.,
 457 Raimbault, P., and Joux, F., 2012, Carbon fluxes in the Canadian Arctic: patterns and
 458 drivers of bacterial abundance. Production and respiration on the Beaufort Sea margin, *Bio*
 459 *geosci.*, 9, 3679-3692.
- 460 Ortega-Retuerta, E., Frazer, T.K., Duarte, C.M., Ruiz-Halpern, S., Tovar-Sanchez, A., Arrieta, J.M.,
 461 and Reche, I., 2009, Biogeneration of chromophoric dissolved organic matter by bacteria
 462 and krill in the Southern Ocean, *Limnol. Oceanogr.*, 54(6), 1941-1950.
- 463 Peterson, B.J., Holmes, R.M., McClelland, J.W., Vorosmarty, C.J., Lammers, R.B., Shiklomanov,
 464 A.I., Shiklomanov, I.A., and Rahmstorf, S., 2002, Increasing river discharge to the Arctic
 465 Ocean, *Science*, 298, 2171-2173.
- 466 Raymond, P.A., McClelland, J.W., Holmes, R.M., Zhulidov, A.V., Mull, K., Peterson, B.J., Striegl,
 467 R.G., Aiken, G.R., and Gurtovaya T.Y., 2007, Flux and age of dissolved organic carbon
 468 exported to the Arctic Ocean: A carbon isotopic study of the five largest arctic rivers,

Global. Biogeochem. Cycles., 21, GB4011, doi:10.1029/2007GB002934.

Shen, Y., Fichot, C.G., and Benner, R., 2012, Dissolved organic matter composition and bioavailability reflect ecosystem productivity in the Western Arctic Ocean, Biogeosci., 9, 4993-5005.

Smith, D.C., Azam, F., 1992, A simple, economical method for measuring bacterial protein synthesis rates in seawater using 3H-leucine. Mar Microb Food Webs 6, 107-114.

Suzuki, K.W., Kasai, A., Nakayama, K., and Tanaka, M., 2012, Year-round accumulation of particulate organic matter in the estuarine turbidity maximum: comparative observations in three macrotidal estuaries (Chikugo, Midori, and Kuma Rivers), southwestern Japan, J. Oceanogr., 68, 453-471.

Twardowski, M.S., and Donaghay, P.L., 2002, Photobleaching of aquatic dissolved materials: Absorption removal, spectral alteration, and their interrelationship, J. Geophys. Res., 107(C8), 3091, 10.1029/1999JC000281.

Uitz, J., Huot, Y., Bruyant, F., Babin, M., and Claustre, H., 2008, Relating phytoplankton photophysiological properties to community structure on large scales, Limnol. Oceanogr., 53(2), 614-630.

Yamashita, Y., Nosaka, Y., Suzuki, K., Ogawa, H., Takahashi, K., and Saito, H., 2013, Photobleaching as a factor controlling spectral characteristics of chromophoric dissolved organic matter in open ocean, Biogeosci., 10, 7207-7217, doi:10.5194/bg-10-7207-2013.

Figure captions

Figure 1. Locations of sampling stations for ICESCAPE 2010 (blue crosses), ICESCAPE 2011 (red diamonds), and MALINA (black circles) cruises in the Arctic Ocean. A transect from Kotzebue Sound (KS) to the Chukchi Hotspot (CH) is shown as a black line. Vertical sections of CDOM absorption properties as well as salinity and phaeopigment concentrations along this transect in the intermediate layer (i.e., $30.7 < \text{salinity} < 33.9$) are shown in Figure 5.

Figure 2. Mean sea ice concentration images provided by the using satellite microwave sensor, DMSP SSM/I, during (a) MALINA, (b) ICESCAPE2010, and (c) ICESCAPE2011 cruises. These images were generated by averaging daily images available during each cruise. Sampling stations are also displayed with white circles, yellow crosses, and red diamonds, respectively.

Figure 3. Vertical profiles of (a) CDOM absorption coefficients at 440 nm ($a_{\text{CDOM}}(440)$, m^{-1}) and (b) their spectral slope (S_{CDOM} , nm^{-1}). X-axis for (a) is log-transformed to show variability in both low and high $a_{\text{CDOM}}(440)$ values. Mean profiles of (c) $a_{\text{CDOM}}(440)$ and (d) S_{CDOM} with 10-m intervals. Standard deviations are shown as horizontal bars.

Figure 4. Upper panels: CDOM absorption coefficients at 440 nm as a function of salinity (S) for (a) the whole salinity range and (c) for $S \geq 28$. A linear fit provided by Matsuoka et al. (2012) is shown in grey. Data points along this fit correspond to river-influenced waters. Data points for ice melt waters are shown in the circle in (a). Lower panels: spectral slope of CDOM absorption coefficients, S_{CDOM} as a function of salinity for (b) the whole salinity range and (d) for $S \geq 28$.

Figure 5. Vertical sections of (a) salinity, CDOM absorption properties (b) $a_{\text{CDOM}}(440)$ and (c) S_{CDOM} , and (d) phaeopigment concentrations along the transect from Kotzebue Sound (KS) to the Chukchi Hotspot (CH).

Figure 6. Relationship between S_{CDOM} and (a) bacterial production (BP, $\mu\text{g C m}^{-3} \text{ d}^{-1}$) and (b)

bacterial abundance (BA, cells ml⁻¹).

Figure 7. Biplot of principal component analysis (PCA). The important features of this plot are as follows: 1) direction of each arrow represents contribution to principal component 1 (PC1: x-axis) and 2 (PC2: y-axis) for a given variable and 2) magnitude of an arrow represents the strength of the variable to the components. For example, BP and chl *a* concentrations showed a similar direction, suggesting they are related to each other and to positive PC1. This result is consistent with the direct regression analysis (Figure 6 and Table 1). The positive PC1 reflects production of organic matter (section 3.4). Thus, BP and chl *a* concentrations can be considered as contributors to the production of organic matter. See section 3.4 for details.

Table 1. Summary of the Model II regression analysis for bacterial production (BP, $\mu\text{gC m}^{-3} \text{ d}^{-1}$) and abundance (BA, cells ml⁻¹) as a function of chlorophyll *a* (chl *a*, mg m⁻³) concentrations, spectral slope of CDOM (S_{CDOM} , nm⁻¹), temperature (T, degrees C), salinity, and nitrate (NO_3 , $\mu\text{mol kg}^{-1}$) concentrations. A total of 133 samples were used for each regression analysis.

Parameter	Statistics	Log ₁₀ (BP)	Log ₁₀ (BA)
Log ₁₀ (chl <i>a</i>)	r^2	0.24	0.22
	Slope	0.40	0.15
	<i>p</i> -value	< 0.0001	< 0.0001
S_{CDOM}	r^2	0.20	0.26
	Slope	-169.9	-73.65
	<i>p</i> -value	< 0.0001	< 0.0001
Log ₁₀ (T+2)*	r^2	0.18	0.17
	Slope	0.70	0.26
	<i>p</i> -value	< 0.0001	< 0.0001
Salinity	r^2	0.04	0.10

NO ₃	Slope	0.06	0.04
	<i>p-value</i>	< 0.05	< 0.01
	<i>r</i> ²	0.04	0.05
	Slope	-0.03	-0.01
	<i>p-value</i>	< 0.05	< 0.01

*For conversion to a base 10 logarithm, 2 was added to T.

Table 2. Determination coefficients between bacterial variables (BP or BA) and spectral slope parameters ($S_{275-295}$, $S_{350-400}$, and its ratio S_R) proposed by Helms et al. (2008).

<i>r</i> ²	Log ₁₀ (BP)	Log ₁₀ (BA)
$S_{275-295}$	0.11	0.12
$S_{350-400}$	0.19	0.23
S_R	0.03	0.04

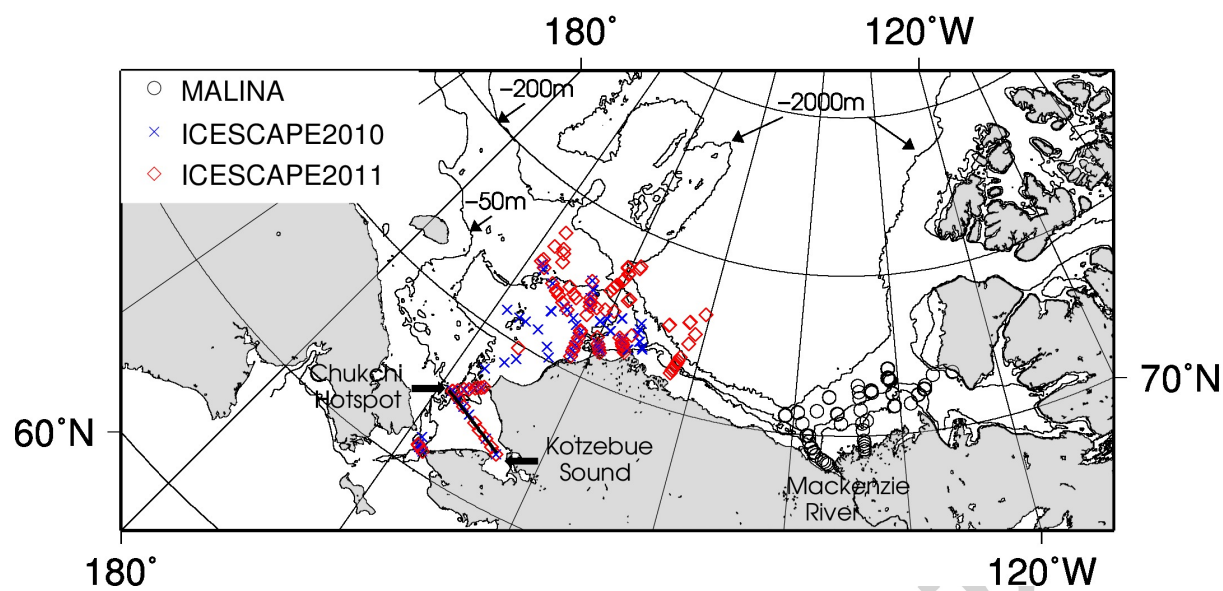


Figure 1

Matsuoka et al.

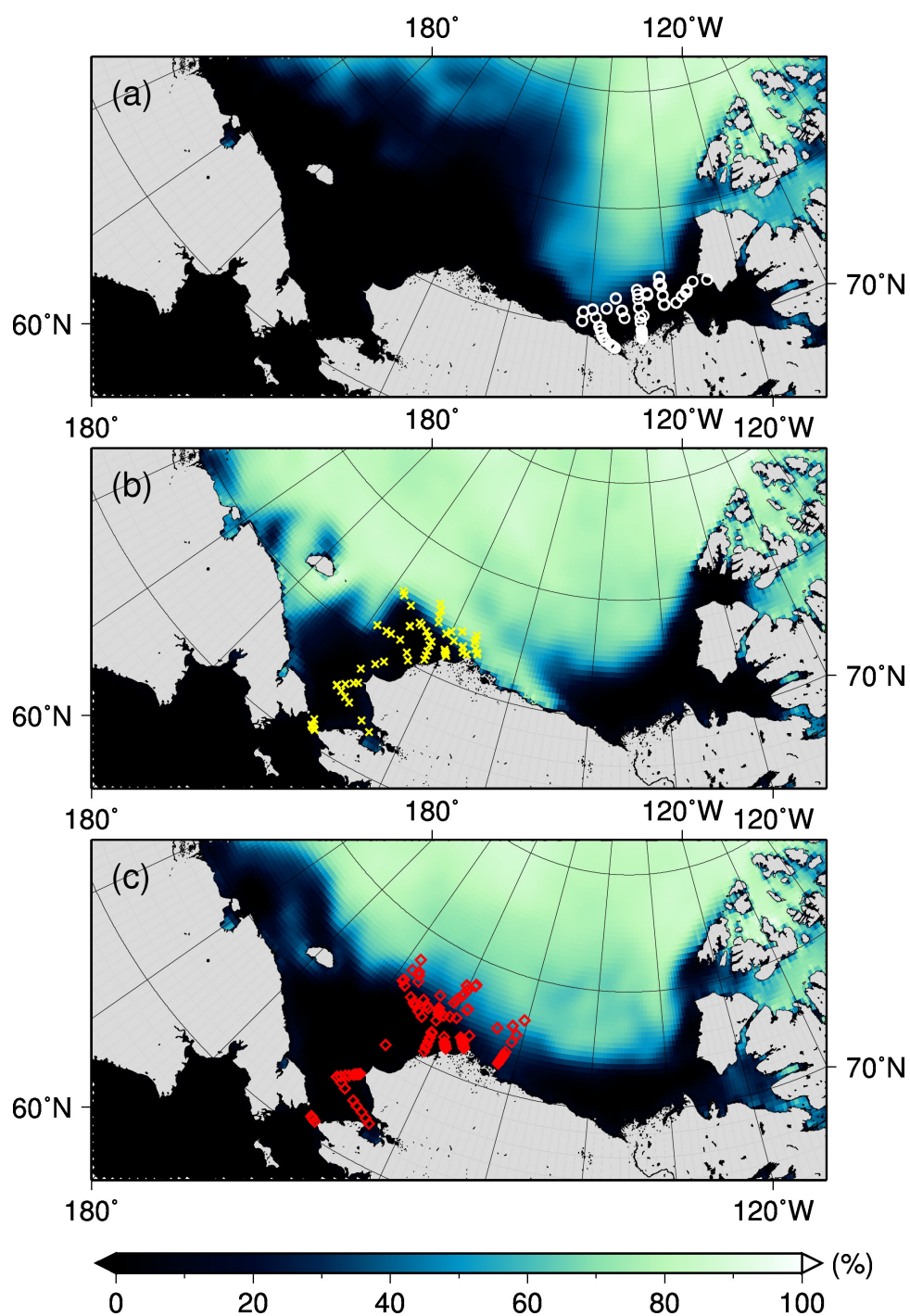


Figure 2

Matsuoka et al.

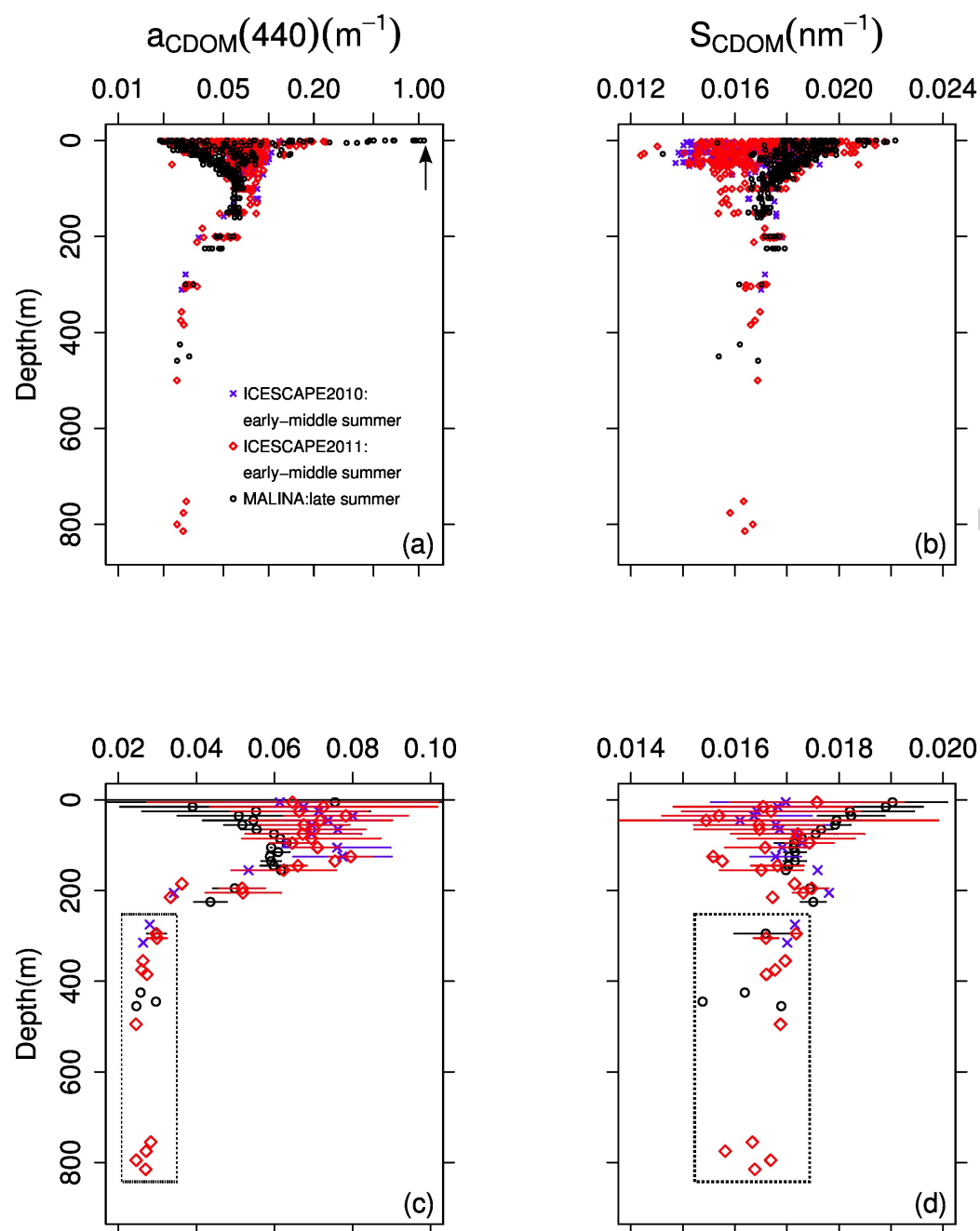


Figure 3

Matsuoka et al.

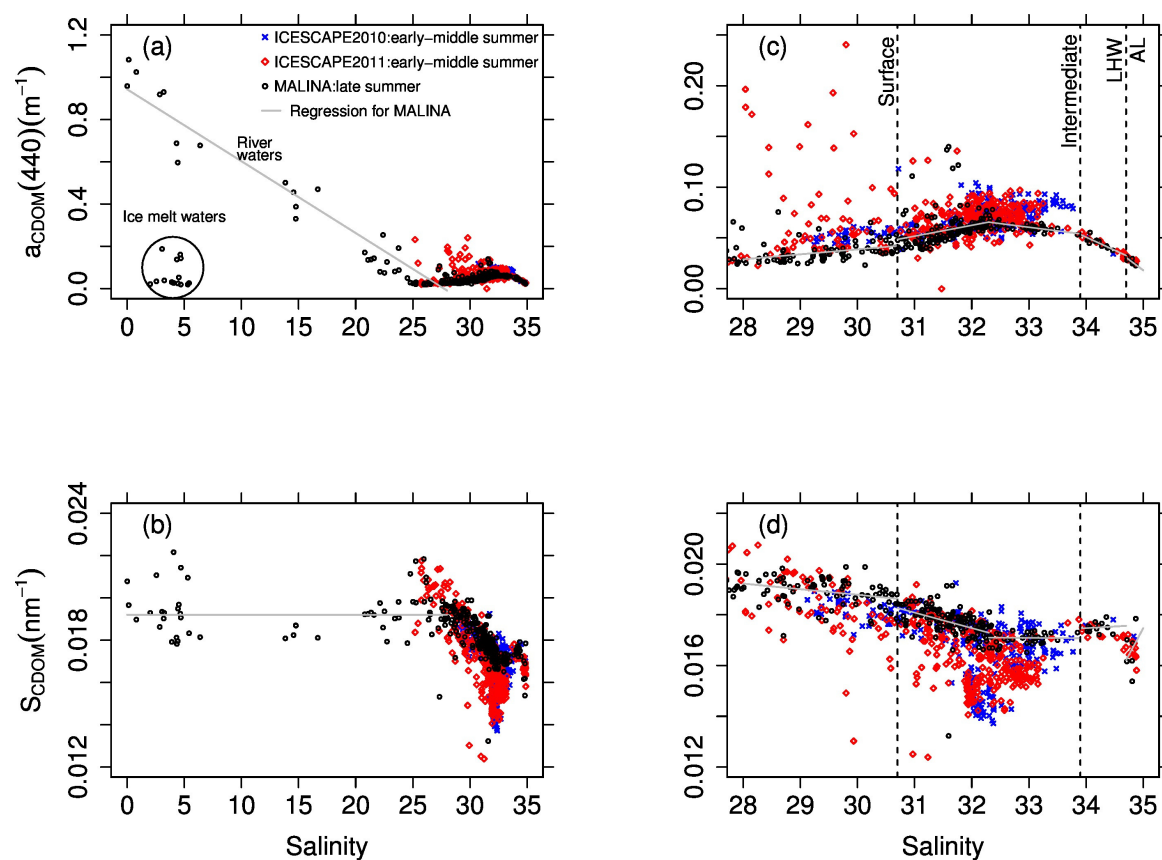


Figure 4

Matsuoka et al.

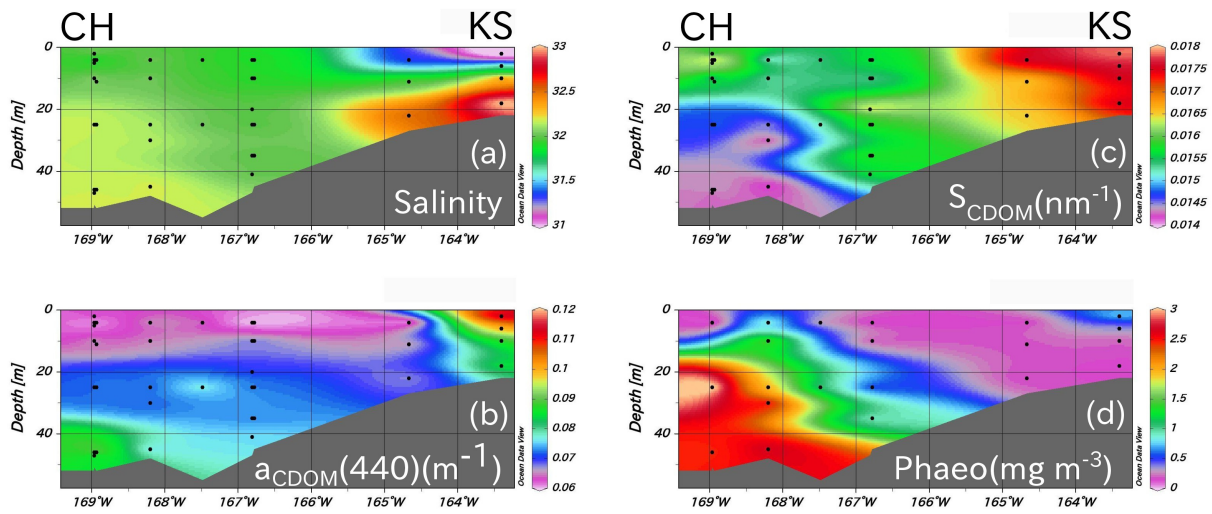


Figure 5

Matsuoka et al.

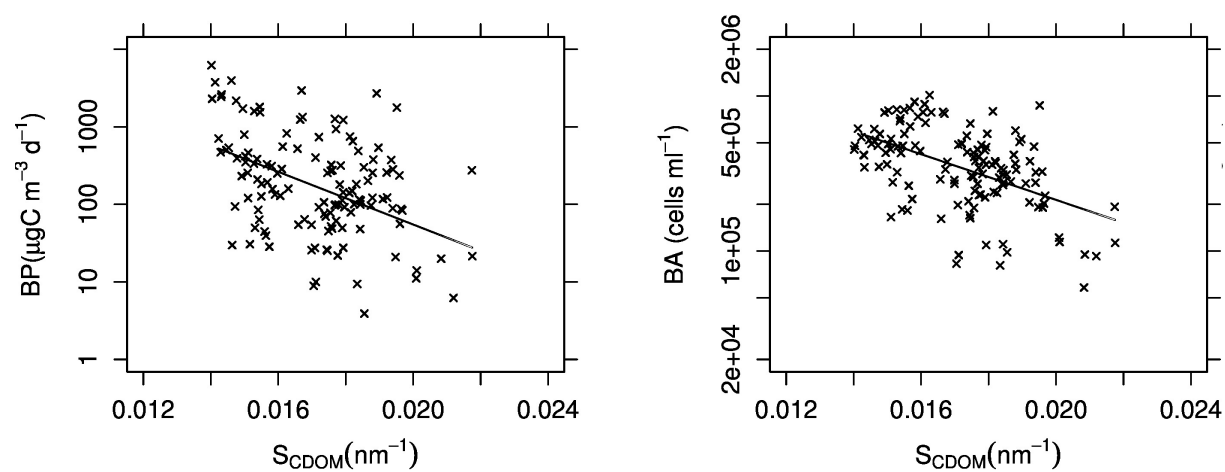


Figure 6
Matsuoka et al.

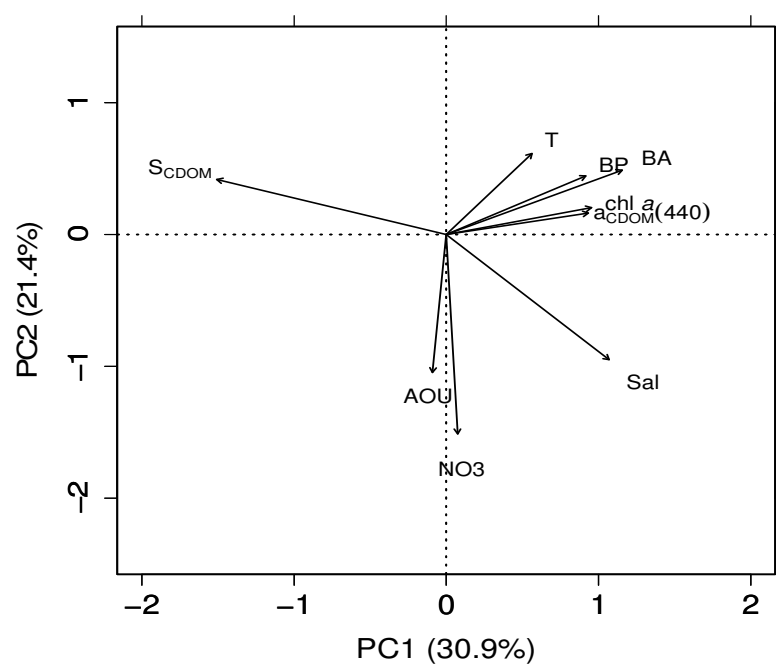


Figure 7

Matsuoka et al.